CHAPTER IV

RESULTS AND DISCUSSION

The aim of this work was to investigate the role of hydrophilic/hydrophobic block lengths in the copolymer-magnetite complex on the properties of the particles, such as stability in water, magnetic properties and drug-entrapment and loading efficiencies. To prepare bilayer surface magnetite nanoparticles, oleic acid as primary surfactant and amphiphilic block copolymer as secondary surfactant were used. The hydrophobic blocks of the amphiphile are thought to physically adsorb onto pre-synthesized oleic acid-coated particles and hydrophilic block provides dispersibility in water and prevents the particles approaching to neighboring particles. The hydrophobic inner shell might be used for efficient entrapping hydrophobic drug for use as sustainable drug release vehicle. Indomethacin, the poorly water-soluble model drug, was thus hypothetically entrapped into the inner hydrophobic shell. Owing to their high surface area-to-volume ratio of nanoparticles, it was envisioned that high drug loading efficiency should be gained. This system also enables for viable tuning of $\overline{M}_n$s of mPEG and polyester blocks to control the degree of hydrophilicity/ hydrophobicity of the copolymers, which definitely affects dispesibility and stability of the particles in water.

Hence, this chapter discusses two main topics as following:

1. Synthesis and characterization of mPEG-polyester copolymer and the stabilization of the copolymer-coated magnetite nanoparticles
2. The use of the copolymer-coated magnetite nanoparticles for entrapment of an indomethacin model drug

Synthesis and characterization of mPEG-polyester copolymer and its stabilization to magnetite nanoparticles

1. Synthesis and characterization of mPEG-polyester copolymer

An example of a ^{1}H NMR spectrum of the copolymer prepared from malonic acid (Ma), 1,6-hexanediol (He) and mPEG 2,000 g/mol (M2) is shown in

Figure 23c, while its precursors, 1,6-hexanediol and mPEG, are illustrated in Figure 23a and 23b, respectively. The formation of ester linkages was confirmed by the appearance of the signal at 4.13 ppm (*a'*) corresponding to methylene protons adjacent to the ester linkage. In good agreement with ^{1}H NMR results, FTIR spectra show the shift of a relatively broad signal at 1706 cm^{-1}, corresponding to the C=O stretching vibration of malonic acid, to a sharp signal at 1732 cm^{-1}, corresponding to the C=O stretching vibration of the polyester (Figure 24). ^{1}H NMR and FTIR spectra of the copolymers having different copolymer compositions show similar indication of the formation of ester linkages as illustrated in Appendix B.

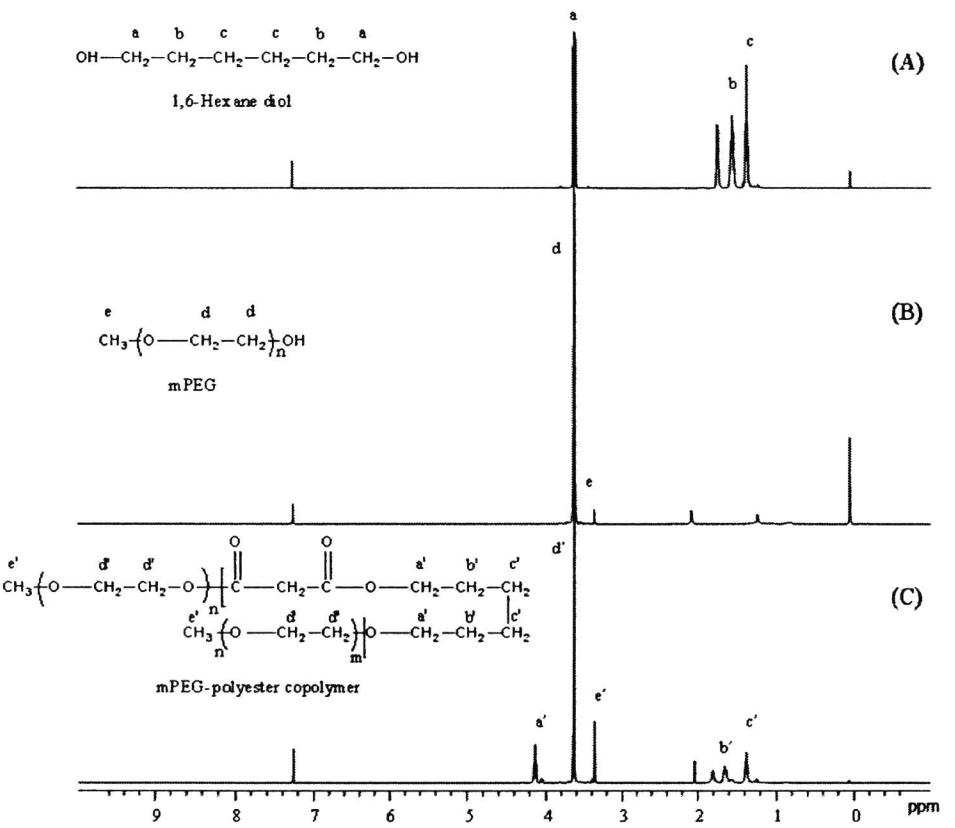

Figure 23 ^{1}H NMR spectra of (A) 1,6-hexanediol, (B) mPEG 2,000 g/mol and (C) mPEG-polyester copolymer (Ma/He/M2 copolymer)

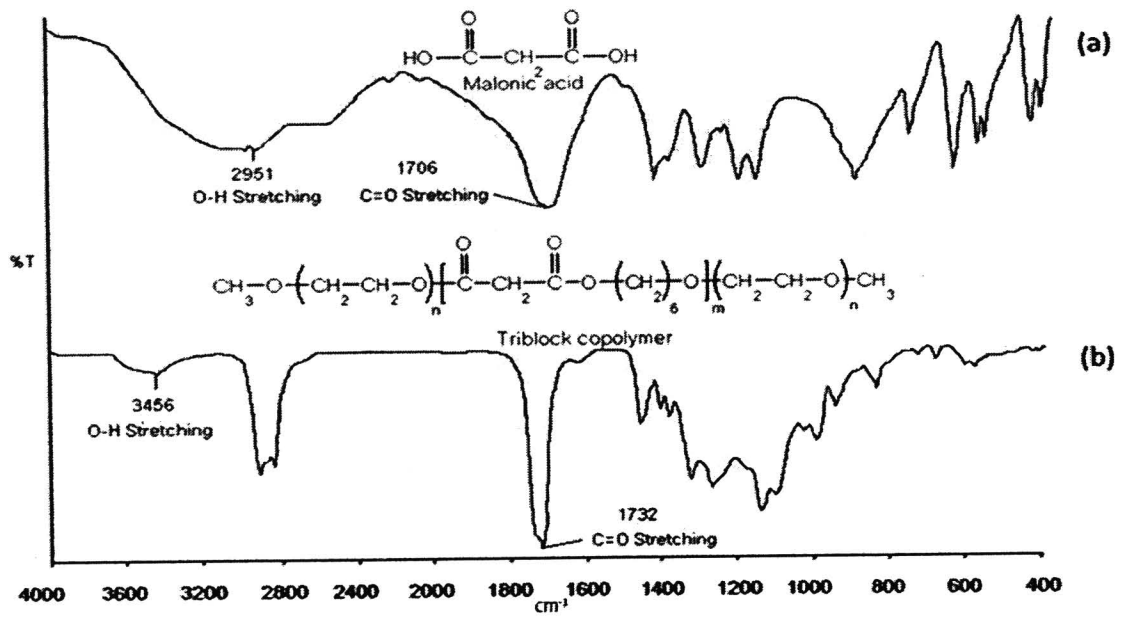

Figure 24 FTIR spectra of (a) malonic acid and (b) mPEG-polyester copolymer (Ma/He/M2 copolymer)

Because mPEG is monofunctional oligomer, it should also function as an endcapping agent and essentially control the molecular weight of the polyester block. It is therefore envisioned that diblock copolymers of hydrophobic polyester block and hydrophilic mPEG block should be obtained as a major product. The condensation of the polyester blocks was performed at high temperature under reduced pressure in acidic condition for 24 h to reach the reaction equilibrium. An example of GPC chromatograms of Ma/He/M2 copolymer and mPEG 2,000 g/mol oligomer are illustrated in Figure 25, showing the increase of the molecular weight and its distribution upon the reaction completed. GPC chromatograms of Me/Et/M5 copolymer and mPEG 5,000 g/mol oligomer are illustrated in Figure 26, showing the increase of the molecular weight and its distribution upon the reaction completed. From Table 2, the targeted $\overline{M}_n$ of the copolymer was estimated from the combination of $\overline{M}_n$ of mPEG and the targeted $\overline{M}_n$ of polyester, while the obtained $\overline{M}_n$ of the copolymer was calculated from the combination of $\overline{M}_n$ of mPEG and $\overline{M}_n$ of the polyester estimated from ^{1}H NMR spectra based on $\overline{M}_n$ of mPEG. Namely, $\overline{M}_n$ of the polyester blocks was estimated from the methylene protons adjacent to the ester

linkage in each repeating unit (-(C=O)O-C<u>H</u>$_2$-, 4.13 ppm, signal *a'* in Figure 24) in conjunction with the methylene protons in the repeating unit of mPEG (-CH$_2$C<u>H</u>$_2$O-, 3.64 ppm, signal *d'* in Figure 23). ^{1}H NMR spectra of the copolymers with various block lengths exhibited different integration ratios of signal *d'* to signal *a'*, which thus affected $\overline{M}_n$ of each block in the copolymers. An example of the calculation of the molecular weights from 1H NMR is shown in Appendix A-4.

In all cases, the calculated $\overline{M}_n$s were lower than those of the estimated values and these were in good agreement with GPC results. This was attributed to the inherently limited monomer conversion of the direct condensation reaction in combination with the fact that this type of reaction is highly sensitive to the stoichiometry of the monomers used in the reaction. Polydispersity indices (PDI) obtained from GPC experiments ranged between 1.12 and 2.35. It was also noticed that $\overline{M}_n$ of the copolymers obtained from the use of ethylene glycol (Et) monomer were relatively lower than those of other copolymers. This was attributable to some loss of ethylene glycol monomers at the early state of the condensation because this reaction was performed at high reaction temperature (140°C) under reduced pressure (bp of ethylene glycol = 196°C).

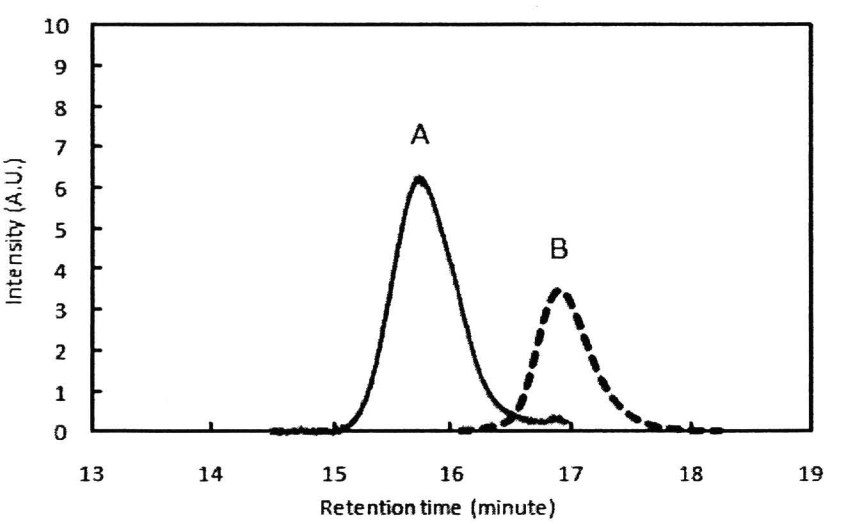

Figure 25 GPC chromatograms showing molecular weight distributions of (A) Ma/He/M2 copolymer and (B) mPEG 2,000 g/mol oligomer

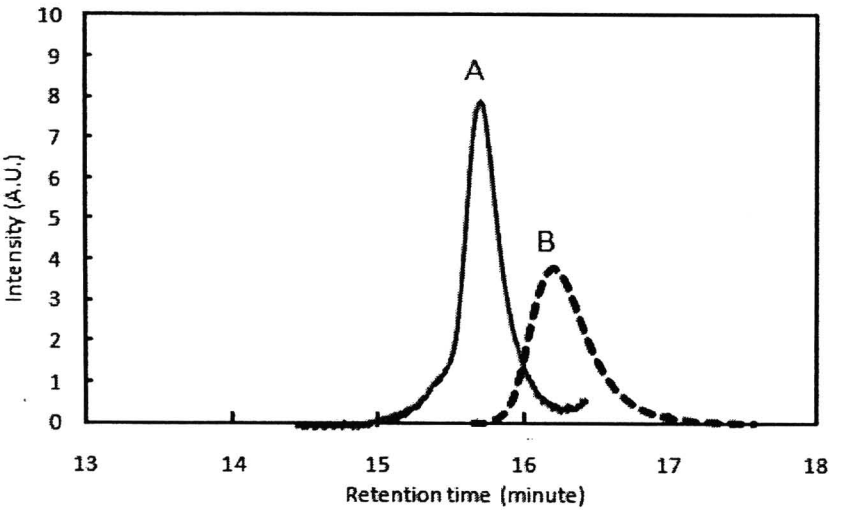

Figure 26 GPC chromatograms showing molecular weight distributions of (A) Me/Et/M5 and (B) mPEG 5,000 g/mol

Table 2 Molecular weights and polydispersities of mPEG-polyester copolymers

Copolymer name [a]	$\overline{M}_n$ of each block (mPEG-polyester) (g/mol)	Targeted $\overline{M}_n$ [b] of copolymer (g/mol)	$\overline{M}_n$ [c] of copolymer from ^{1}NMR (g/mol)	$\overline{M}_n$ [d] of copolymer from GPC (g/mol)	polydispersity index[d] (PDI)
Ma/He/M2	2K-5K	7,000	6,200	5,538	1.56
Ma/Et/M2	2K-5K	7,000	3,400	3,801	1.74
Me/He/M2	2K-5K	7,000	5,850	3,735	1.49
Me/Et/M2	2K-5K	7,000	3,650	3,449	1.12
Ma/He/M5	5K-5K	10,000	6,650	6,967	1.17
Ma/Et/M5	5K-5K	10,000	5,500	6,376	1.16
Me/He/M5	5K-5K	10,000	6,250	4,917	2.35
Me/Et/M5	5K-5K	10,000	5,700	7,028	1.21

[a]Ma = malonic acid, Me = maleic acid, He = 1,6-hexanediol, Et = ethylene glycol, M2 = mPEG 2,000 g/mol and M5 = mPEG 5,000 g/mol

[b]calculated from ($\overline{M}_n$ of mPEG + targeted $\overline{M}_n$ of polyester)

[c]calculated from ($\overline{M}_n$ of mPEG + obtained $\overline{M}_n$ of polyester), where $\overline{M}_n$ of polyester estimated from ^{1}H NMR based on $\overline{M}_n$ of mPEG

[d]estimated from GPC

2. Effect of the copolymer compositions and concentrations on stability of the particles

The as-synthesized mPEG-polyester copolymers having various compositions and block lengths were used as polymeric surfactants of magnetite nanoparticles. It was envisioned that the stabilizing mechanism of the particles in water was the physi-sorption of hydrophobic polyester block to the particle surfaces pre-coated with an oleic acid primary surfactant and having hydrophilic mPEG tail blocks to provide steric repulsions in aqueous dispersions. The particle surfaces thus possessed hydrophobic inner shells of oleic acid-polyester layers and hydrophilic corona of mPEG layers.

Preliminary experiments were performed to select suitable copolymer compositions that can effectively stabilize the particle in water. The pre-synthesized oleic-coated magnetite nanoparticles were dispersed in 5% of the copolymers in water. Appearance of dispersions is shown in Table 3 and Figure 27. It is noticed that magnetite nanoparticles stabilized by polyester made of 1,6-hexanediol (abbreviated as He) regardless of types of diacid and $\overline{M}_n$ of mPEG resulted in good dispersibility in water, as indicated by only a slight precipitant observed. In addition, the color of the dispersion in black is another indication of well dispersed nanoparticles in water (Figure 27). It was rationalized that degree of hydrophobicity of C6 of 1,6-hexanediol might be suitable for physical adsorption to surface of the oleic acid-precoated magnetite nanoparticles.

It should be noted that the mPEG-polyester copolymers comprised of mPEG (2,000 g/mol and 5,000 g/mol), malonic acid and 1,12-dodecanediol were also synthesized. However, their poor solubility in water due to the presence of C12 of 1,12-dodecanediole in polyester block limited the efficiency in stabilization of the particles in aqueous dispersions. From the preliminary results of their dispersibility in water, Ma/He/M2 copolymer (entry 1) and Ma/He/M5 copolymer (entry 5) were thus selected for further investigations.

Table 3 Effect of the copolymer composition on stability of the particles

Sample number	Type of copolymer	Appearance	
		precipitation	color of the dispersion
1	Ma/He/M2	slightly	black
2	Ma/Et/M2	moderately	red
3	Me/He/M2	slightly	black
4	Me/Et/M2	significantly	yellow
5	Ma/He/M5	slightly	black
6	Ma/Et/M5	moderately	red
7	Me/He/M5	slightly	black
8	Me/Et/M5	moderately	red

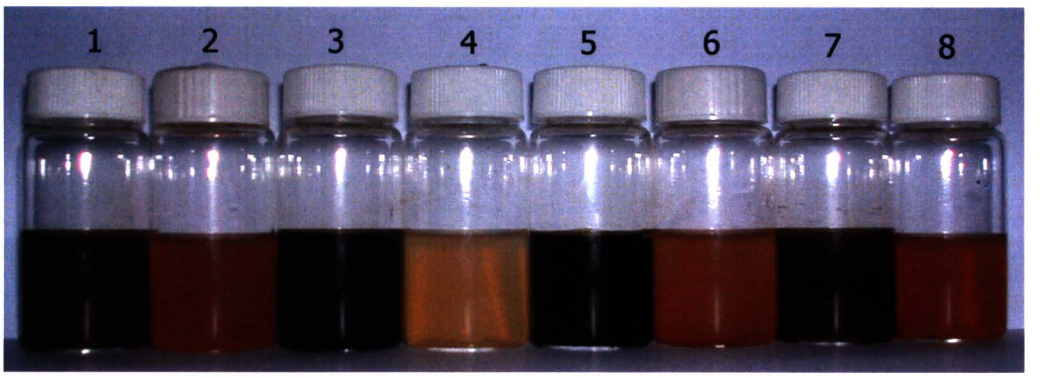

Figure 27 Appearance of the copolymer-stabilized magnetite nanoparticle in aqueous dispersions after removing precipitant by centrifugation. Number 1-8 correspond to the sample numbers in Table 3. Black color of sample 1, 3, 5 and 7 is indicative of good dispersibility of the particles in water

The effect of the copolymer concentrations on dispersibility of the stabilized particles in aqueous dispersions was also investigated. Figure 28 shows transferring efficiencies of the stabilized particles from hexane to water phases as a function of the copolymer concentrations (0.01 to 5 wt% of the copolymers in water).

Increasing copolymer concentrations seemed to enhance transferring efficiencies of the particles due to sufficient amounts of the copolymers applied. When the copolymer concentration lower than 0.01% was used for the particle stabilization, insignificant number of transferring efficiency was obtained. In addition, the copolymers containing 5,000 g/mol mPEG tended to significantly promote the particle dispersibility in water as compared to the ones having 2,000 g/mol mPEG due to relatively high degree of hydrophilicity of 5,000 g/mol mPEG. Therefore, the Ma/He/M5 mPEG-polyester copolymer (entry 5 in table 3) would be then used for other experiments to investigate effect of its concentrations in the aqueous dispersion on properties of the copolymer-magnetite complexes.

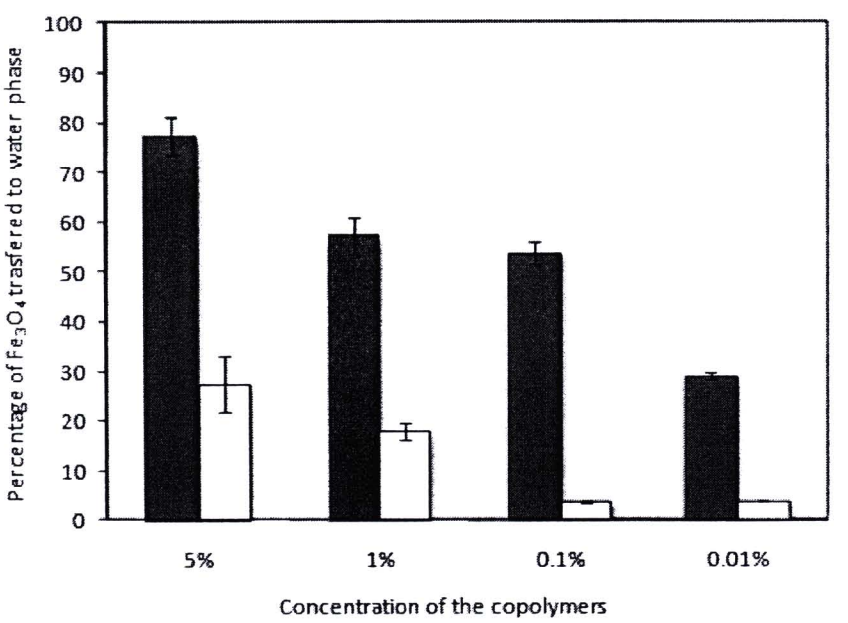

Figure 28 Transferring efficiencies of magnetite nanoparticle from hexane to aqueous phases after stabilization with Ma/He/M5 (■) and Ma/He/M2 (□) copolymers

Concentrations of the dispersible particles (% wt/v) in water were another indicative of the transferring efficiency of the particle from hexane to water phases. Figure 29 shows magnetite concentrations that can be dispersible in water as a function of the copolymer concentrations used. In good agreement with the transferring efficiency plot in Figure 29, increasing the copolymer concentrations

seemed to enhance percentages of the water dispersible particles with the maximum concentration of 6.0 %wt/v (6.0 g/ml).

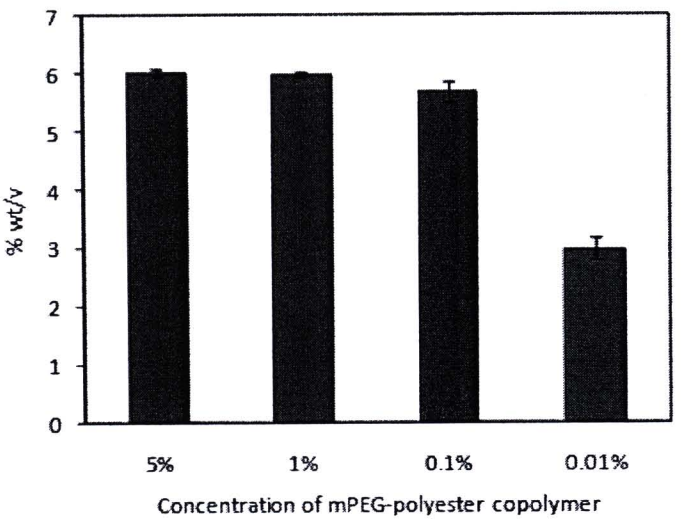

Figure 29 Concentrations of magnetite nanoparticles stabilized with Ma/He/M5 copolymer in aqueous dispersions

Because the stabilizing mechanism of the complexes in water involved physi-sorption of hydrophobic polyester blocks to oleic acid pre-coated magnetite surfaces, their stability in water was thus concerned. Magnetite concentrations in the dispersions were monitored as a function of time using various copolymer concentrations (0.001-1 %). The dispersions were centrifuged (3000 rpm) once a week to precipitate unstable particles or large aggregate that may arise and percent magnetite in the supernatant was analyzed *via* AAS technique. Figure 30 shows the concentrations of the particles remaining dispersible in water after 1, 2 and 4 weeks as compared to their initial concentrations. The initial concentrations of the dispersible particles in water were strongly dependent on the copolymer concentrations used. In general, the concentrations of magnetite in water decreased about 18-35% in the first week and continuously dropped to about 50% after four weeks, depending on the copolymer concentrations used. The dispersions containing high magnetite concentrations exhibited high tendency of particle aggregation (about 35% particle aggregation in the first week) due to the great proximity of each particle in the

dispersion, resulting in a significant drop of the percentage of the dispersible particles. The dispersions with diluted particle concentrations showed a good stability in water with less than 18% of particle aggregation after one week. However, about 50% of particle aggregation was observed after four weeks of their preparation, indicating that these complexes might be suitable for short-term uses. The decrease of the dispersible particles in water was attributable to redissolution of the copolymers in the complex to the solution.

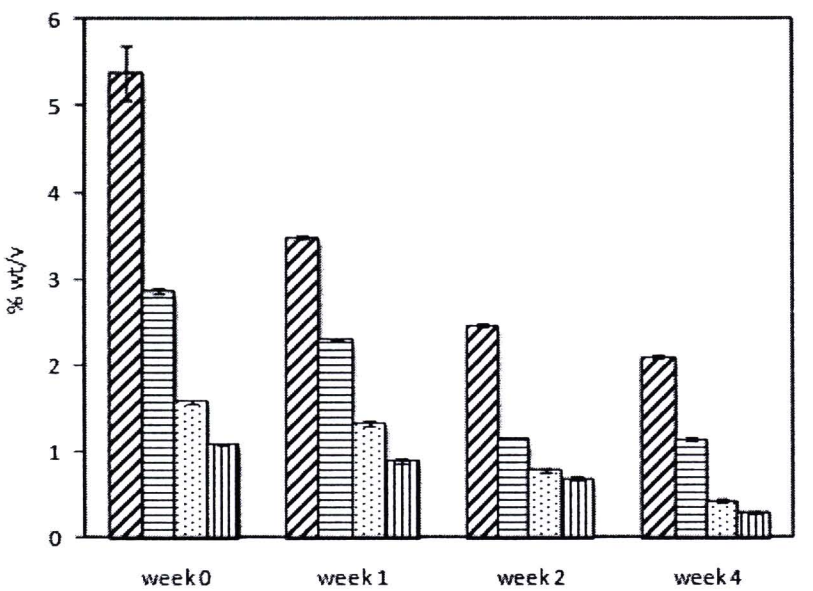

Figure 30 Stability of magnetite nanoparticles stabilized with Ma/He/M5 mPEG-polyester copolymer having 1% (▨), 0.1% (▤), 0.01% (▦) and 0.001% (▥) in water

3. Determination of particle size and size distribution by transmission electron microscopy (TEM)

Particle size and size distribution of the stabilized particles were investigated using transmission electron microscopy (TEM). Figure 31 and 32 show representative TEM images and size distribution of the magnetite-copolymer complex with the use of 1.0 and 0.01 wt% Ma/He/M5 mPEG-polyester copolymer concentrations as a surfactant in water. The particle size ranged between 8 and 14 nm in diameter with the average of approximately 10 nm. The particles with the use of 1

wt% copolymer in water as a surfactant showed a good dispersibility in water without nano-aggregation observed. When low concentrations of the copolymer (0.01 or 0.001 %) were used, similar distribution of the particle was observed with the existence of some nanoclusters. Size of the clusters was about 100 nm in diameter with about 70 nanoparticles in a cluster. The occurrence of these nanoclusters was attributable to the insufficient concentration of the copolymer for stabilization of the particles in the dispersions.

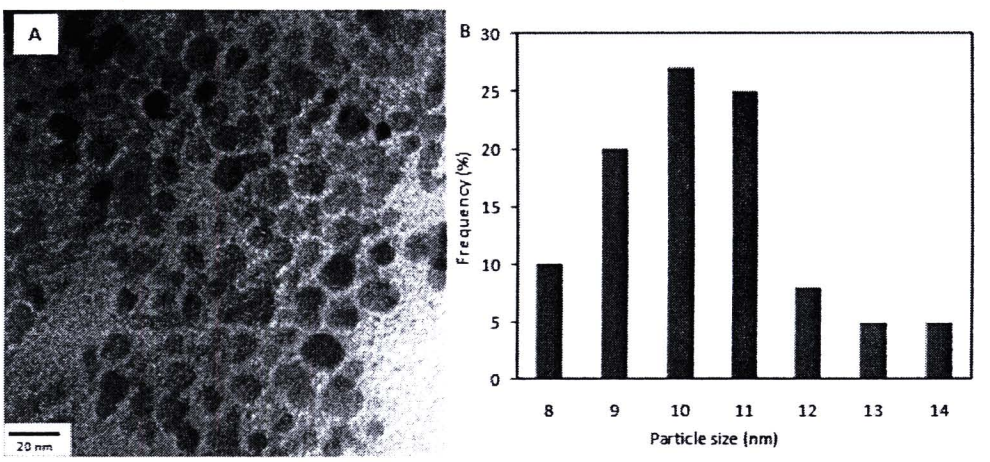

Figure 31 (A) TEM bright field image of magnetite with the use of 1 % Ma/He/M5 mPEG-polyester copolymer in water as a surfactant and (B) particle size distribution with average particle size of 10 nm in diameter

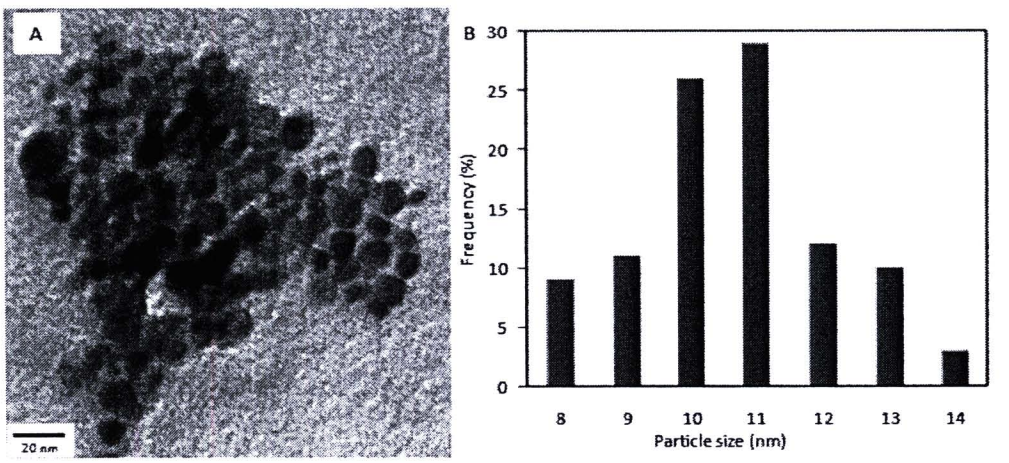

Figure 32 (A) TEM bright field image of magnetite with the use of 0.01 % Ma/He/M5 mPEG-polyester copolymer in water as a surfactant and (B) particle size distribution with average particle size of 10 nm in diameter

4. Determination of the composition in the copolymer-magnetite complex via thermogravimetric analysis (TGA)

Percentages of magnetite core and copolymer shell in each complex were determined *via* a TGA technique. Bare magnetite nanoparticle manifested a weight loss between 200 and 230°C with 93% char yield (Figure 33). It was assumed that percent weight residual was the weight of the iron oxide core that was completely oxidized at 600°C, while the observed weight loss was attributed to the desorption of the absorbed ammonium salt at high temperature [51]. Therefore, in other complexes, percent weight residual would be normallized with a 0.93 factor (% char yield of bare magnetite at 600°C) (Table 4). To determine percentage of oleic acid in each complex, the ratio of magnetite to oleic acid in the oleic acid-coated particle was calculated (2.4:1, respectively), and this ratio was used to calculate percent oleic acid in other complexes. The composition of the copolymer-coated particle was estimated in a similar fashion by assuming that the total composition of all components in the complex was 100%. An example of the calculation is shown in Appendix A-5. TGA thermograms of the copolymer-magnetite complexes showed consistent weight loss ranging between 230 and 520°C (Figure 33), attributed to the decomposition of

organic components including the copolymers and oleic acid complexing to the particle surface. Percentages of the copolymer (48-53%) and magnetite (33-37%) in each complex (Table 4) were similar to each other, indicating that the composition of the dispersible complexes was not dependent on the copolymer concentration used. The copolymer concentrations, on the other hand, played an important role on transferring efficiency of the particles from organic to water phases previously discuss in Figure 28 and 29.

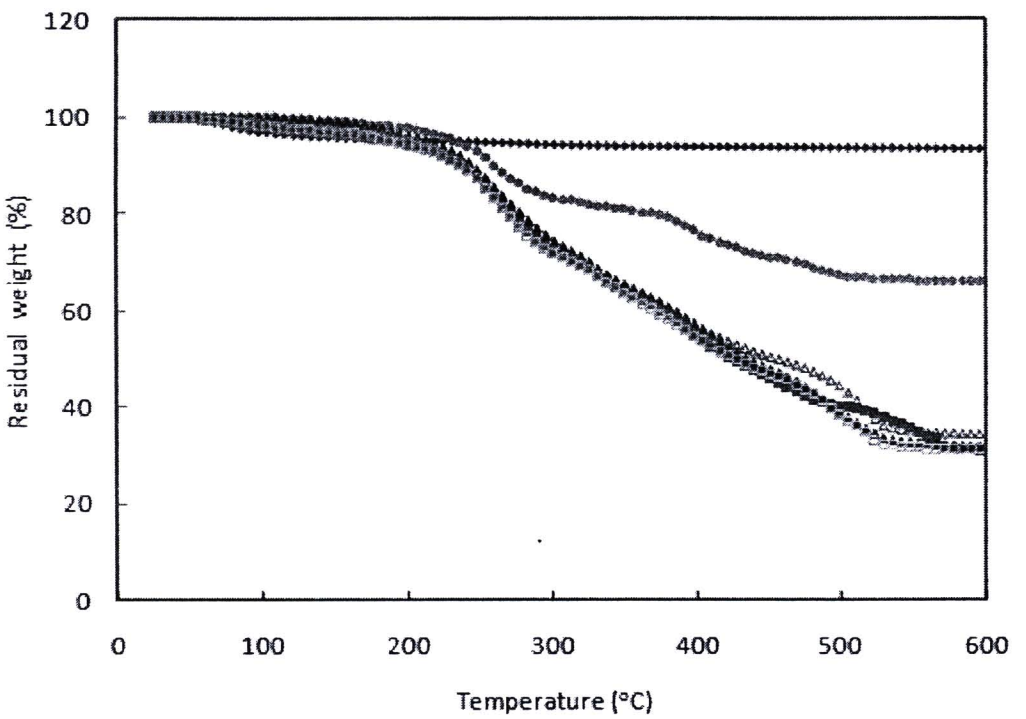

Figure 33 TGA thermograms of bare magnetite (▲), oleic acid-coated magnetite (●), magnetite coated with 1% (□), 0.1% (■), 0.01% (△), and 0.001% (◆) of Ma/He/M5 mPEG-polyester copolymer

Table 4 The compositions of the copolymer-magnetite complexes

	Char yield (%)[a]	Composition in the complexes (%)[d]		
		Fe_3O_4[b]	Oleic acid	Copolymer
Bare magnetite	93	100	-	-
Oleic acid-coated magnetite	66	71[c]	29[c]	-
Copolymer-coated magnetite				
1%	31	33	14	53
0.1%	32	34	14	52
0.01%	34	37	15	48
0.001%	31	33	14	53

[a]Assumimg that char yield is the %wt of iron oxide completely oxidized at 600 °C

[b]Assuming that all iron oxides are in the form of Fe_3O_4 at ambient temperature.

% Fe_3O_4 is % char yield normalized with 0.93 factors (%char yield of bare magnetite)

[c]Ratio of Fe_3O_4 to oleic acid is 2.4 :1 and this is used to calculate their ratio in other complexes

[d]Total compositions of all components in the complexes are 100%

5. Determination of magnetic properties of the copolymer–magnetite complex via vibrating sample magnetometry (VSM)

A representative hysteresis curve of the complex with the use of 1 wt% copolymer was shown in Figure 34. It exhibited superparamagnetic properties at room temperature as indicated by the absence of reminance and coercivity upon removing an external applied magnetic field with saturation magnetization (M_s) about 40 emu/g Fe_3O_4. Other complexes having other copolymer concentrations or without copolymer (bare magnetite) also showed similar magnetic behavior and M_s values, indicating that the presence of the copolymers in the complexes did not affect magnetic properties of the particles.

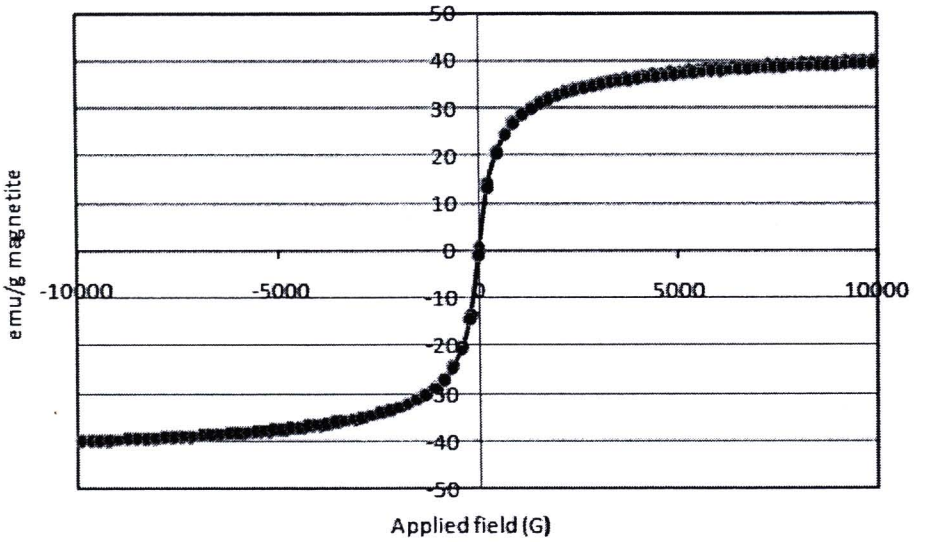

Figure 34 A *M-H* curve of magnetite nanoparticle stabilized with 1% of Ma/He/ M5 mPEG-polyester copolymer

The use of the copolymer-coated magnetite nanoparticle for entrapment of indomethacin model drug

The purpose of this part was to investigate the effect of polyester structure in the inner shell of the bilayer surface of the particles on entrapment efficiency, loading efficiency and releasing behavior of a model compound in the polyester-magnetite complex vehicles. Indomethacin was selected in this experiment because it showed fair solubility in phosphate buffer solution (PBS) which was used as a dialysis releasing media. In addition, its λ_{max} also shows a distinctive absorbance signal in UV-Visible spectrophotometry experiments. Therefore, it was hypothesized that the hydrophobic drug would partially partition in the inner hydrophobic shell of polyester layer on the particle surface, while hydrophilic mPEG block provided steric repulsion and water dispersibility. It is interesting to investigate the influence of saturated and unsaturated structures in the polyester inner shells on the drug entrapment and loading efficiencies of the particles. Crosslinked structure of the unsaturated polyester inner shell was anticipated to sustain or inhibit the desorption of the entrapped drug from the particle surface (Figure 35).

Therefore, there are three types of the mPEG-polyester copolymers used in this experiment: saturated mPEG-polyester copolymer, mPEG-unsaturated polyester copolymer and mPEG-crosslinked polyester copolymer (Figure 36). From the preliminary results in Chapter 4.1, it was found that Ma/He/M5 copolymer seemed to be a suitable one for stabilization of the particles. Therefore, three types of copolymers used in this part were thus based on the Ma/He/M5 copolymer structure. The particles coated with saturated Ma/He/M5 copolymer was designated as "sat-coated particle", while the particles coated with the unsaturated copolymer (5% maleic acid and 95% malonic acid in the polyester structure) was designated as "unsat-coated particle". The unsaturated polyester moiety on the particle surface can be radically crosslinked; the particles were designated as "crosslinked-coated particle".

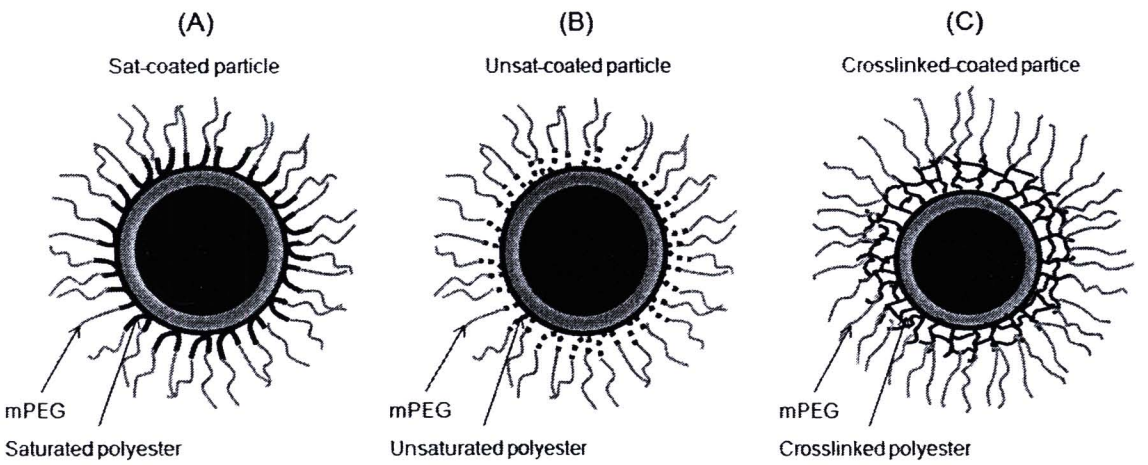

Figure 35 (A) Sat-coated particle (mPEG-saturated polyester-coated particle), (B) Unsat-coated particle (mPEG-unsaturated polyester-coated particle) and (C) Crosslinked-coated particle (mPEG-crosslinked polyester-coated particle)

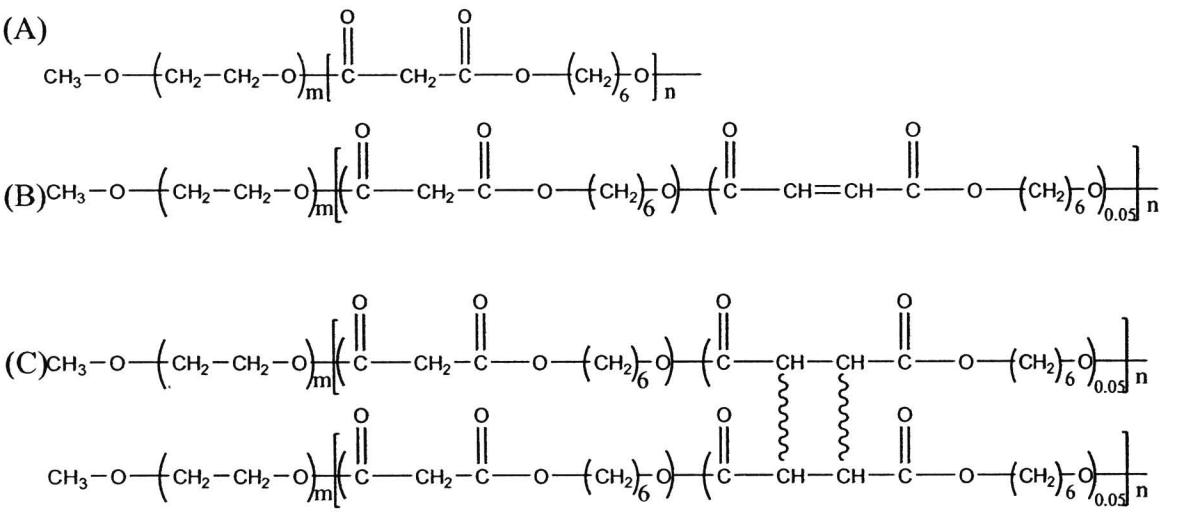

Figure 36 Chemical structures of (A) mPEG-saturated polyester copolymer, (B) mPEG-unsaturated polyester copolymer and (C) mPEG-crosslinked polyester copolymer

1. Characterization of mPEG-polyester copolymer and the copolymer-coated magnetite nanoparticle

^{1}H NMR spectra of mPEG-saturated polyester copolymer and mPEG-unsaturated polyester copolymer are shown in Figure 37. The formation of ester linkages was confirmed by the appearance of the signal at 4.13 ppm (signal *a*) corresponding to methylene protons adjacent to the ester linkage. In the spectrum of mPEG-unsaturated polyester copolymer (Figure 37B), the signal at 6.27 ppm (signal *f*) corresponding to the vinylic protons indicated the presence of unsaturated moiety in the copolymer. FTIR spectra of mPEG-saturated polyester copolymer and mPEG-unsaturated polyester copolymer are illustrated in Figure 38. Due to the small amount of C=C linkages in the unsaturated polyester in the copolymer, the signal belonging to C=C bonds (1,680-1,620 cm^{-1}) was not obviously apparent.

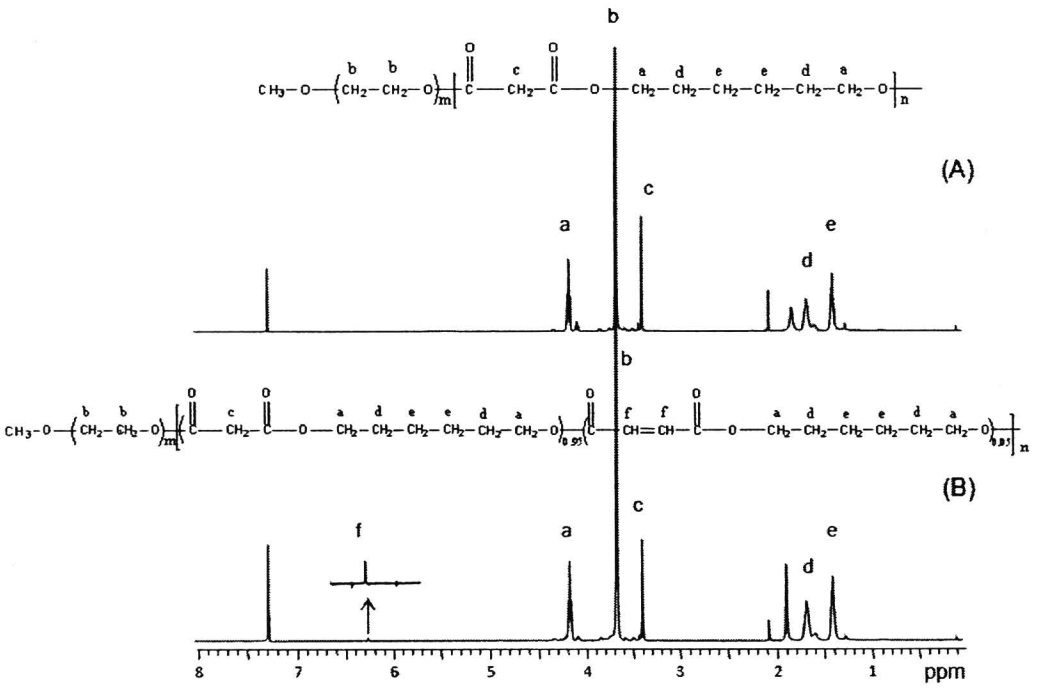

Figure 37 ^{1}H NMR spectra of A) mPEG-saturated polyester copolymer and B) mPEG-unsaturated polyester copolymer

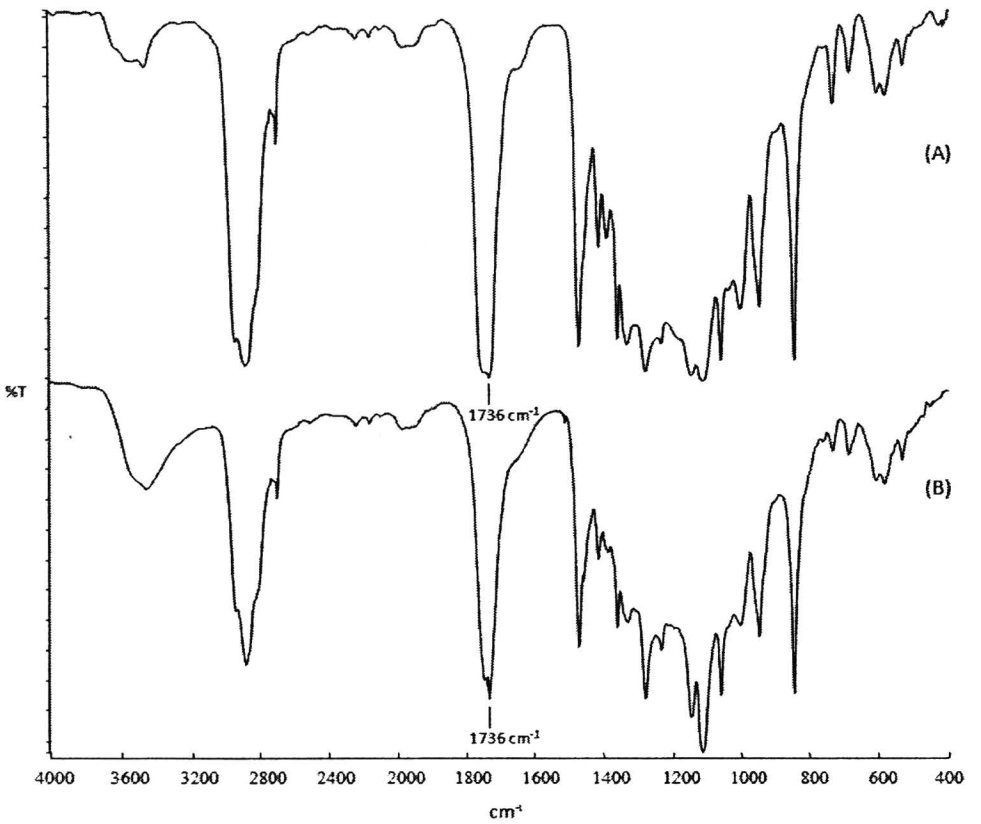

Figure 38 FTIR spectra of (A) mPEG-saturated polyester copolymer and (B) mPEG-unsaturated polyester copolymer

The as-prepared mPEG-polyester copolymers, both saturated and unsaturated ones, were then used as steric stabilizers for magnetite nanoparticles and they were called sat-coated particle and unsat-coated particle, respectively. It was envisioned that the particles were coated with bilayer surface of hydrophobic inner layer due to polyester blocks and hydrophilic corona due to mPEG blocks. The hydrophobic inner shell containing unsaturated polyester can be chemically crosslinked to obtain crosslinked-coated particle. FTIR spectra of these three types of the particles are shown in Figure 39. They show the signal at around 1,712 cm^{-1} corresponding to the C=O stretching vibration of the polyester and at 578 cm^{-1} corresponding to Fe-O bond of magnetite core.

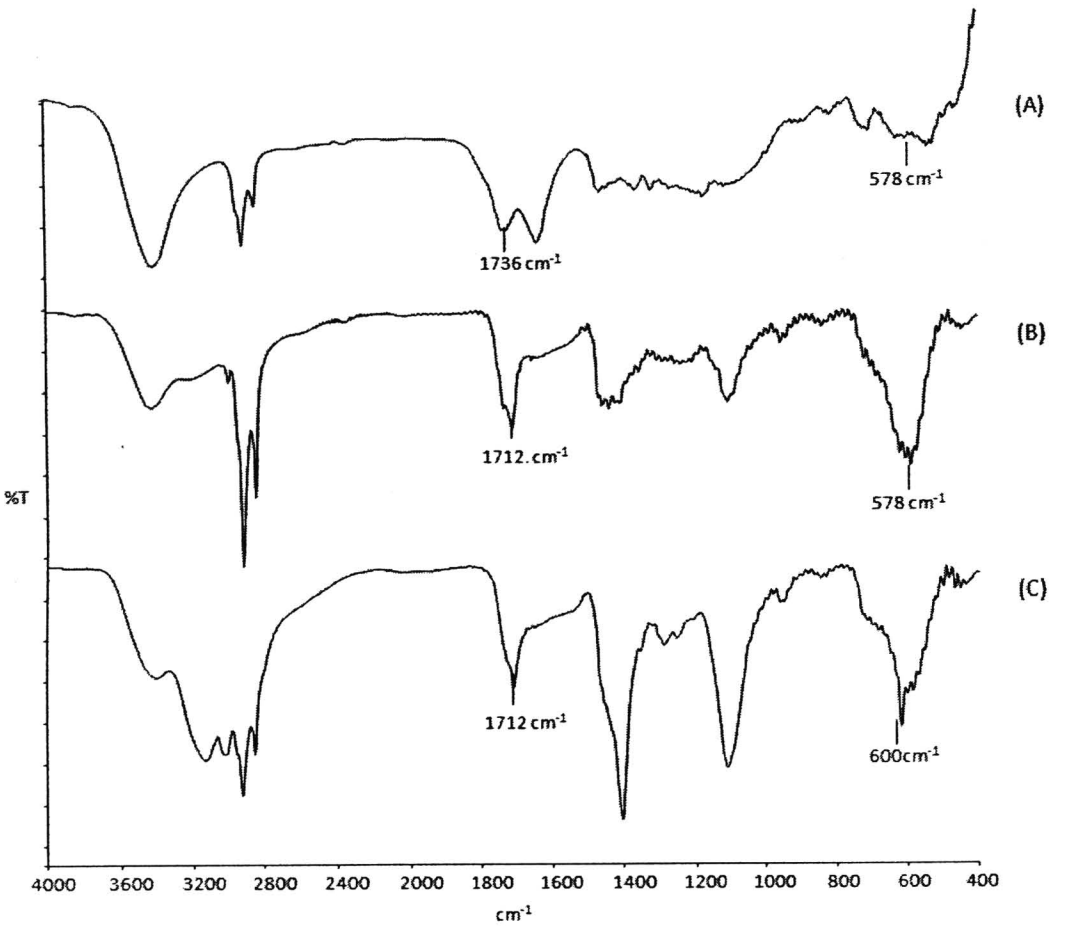

Figure 39 FTIR spectra of (A) sat-coated particle, (B) unsat-coated and (C) crosslinked-coated particle

2. Determination of particle size and size distribution by transmission electron microscopy (TEM)

Particle size and size distribution of the stabilized particles were investigated using transmission electron microscopy (TEM). Figure 40 show representative TEM images of sat-coated particles, unsat-coated particles and crosslinked-coated particles. Sat-coated particles and unsat-coated particles showed a good dispersibility in water without aggregation visually observed. The particle size ranged between 8 and 14 nm in diameter with the average of approximately 10 nm. After crosslinking the inner layer of the particle surface by addition of a radical initiator (KPS), the particles still showed good dispersibility in water without observable aggregation (Figure 40C). It should be noted that the crosslinking reaction

was conducted in a diluted condition to avoid interparticle reaction which resulted in particle agglomeration.

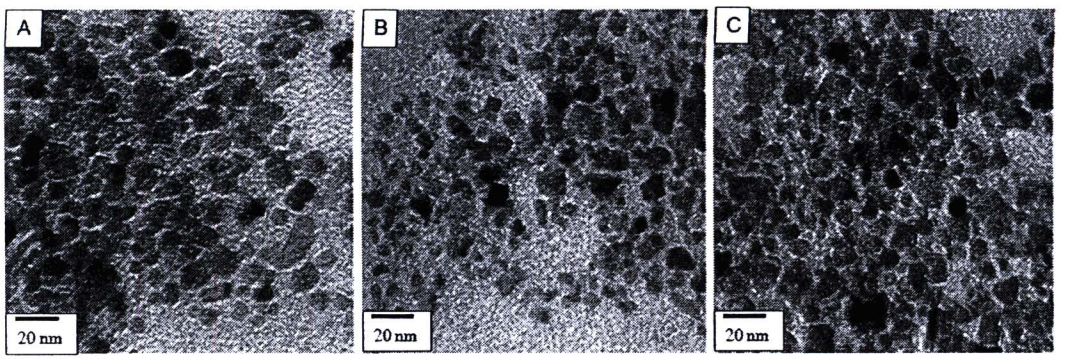

Figure 40 TEM bright field images of (A) sat-coated particles, (B) unsat-coated particles and (C) crosslinked-coated particles

3. Determination of hydrodynamic diameter by photon correlation spectroscopy (PCS)

PCS was conducted to investigate hydrodynamic diameter of the copolymer micelles and their distribution in water and also their complexes with the particles (Table 5). The hydrodynamic diameter ranging between 263 and 289 nm of the copolymers in water was attributed to the size of micelles or aggregation of the copolymer in the solution. In the case of the particles stabilized with the copolymer, the hydrodynamic diameter ranging between 168 and 215 nm was devoted to the size of their complexes with some nanoscale aggregations, which were also observed in TEM experiments (Figure 40). It should be noted that the excess of the copolymer was thoroughly removed from the dispersion by dialysis against water before PCS measurements; micellar structure of the copolymer should not persist in the dispersion. The hydrodynamic diameters of the crosslinked-coated particles were smaller than those of the other two complexes probably due to the contraction of crosslink structure, resulting in the decrease in size of the complex.

Upon loading the drug into the complexes, their hydrodynamic diameters decreased as compared to the ones before drug loading. This was attributed to the

promotion of the structural contraction upon addition of the hydrophobic drug into the complexes.

Table 5 Hydrodynamic diameters of the copolymers in water and their complexes in aqueous dispersions

	Hydrodynamic diameter (nm) (type of mPEG-polyester copolymers used)		
	Saturated	Unsaturated	Crosslinked
Copolymer solution in water [a]	263 ± 4	289 ± 5	-
Copolymer–magnetite complex dispersion [b]	215 ± 3	211 ± 3	168 ± 2
Drug-loaded copolymer–magnetite complex dispersion [c]	182 ± 4	172 ± 4	121 ± 1

[a] The copolymer concentrations for PCS analyses were 0.1 mg/ml.

[b] The excess copolymers were removed by dialysis.

[c] The aggregated drug was removed by centrifugation.

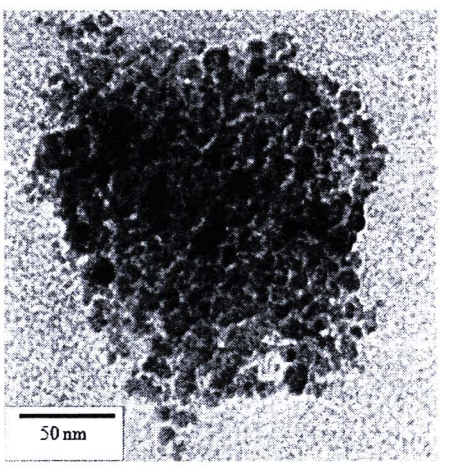

Figure 41 TEM bright field images of unsat-coated particles

4. Determination of the composition in the copolymer-magnetite complex by Thermogravimetric Analysis (TGA)

Percentages of magnetite core and copolymer shell in each complex were determined *via* a TGA technique. Bare magnetite nanoparticle manifested a slight weight loss between 200 and 230°C with 93 % char yield (Figure 42). It was assumed that percent weight residual was the weight of the iron oxide core that was completely oxidized at 600°C, while the observed weight loss was attributed to the desorption of the absorbed ammonium salt at high temperature. Therefore, in other complexes, percent weight residual would be normallized with a 0.93 factor (% char yield of bare magnetite at 600°C) (Table 6). To determine percentage of oleic acid in each complex, the ratio of magnetite to oleic acid in the oleic acid-coated particle was calculated (2.4:1, respectively), and this ratio was used to calculate percentage of oleic acid in other complexes. The composition of the copolymer-coated particle was estimated in a similar fashion by assuming that the total composition of all components in the complex was 100%. An example of the calculations is shown in Appendix A-5. Percentages of the copolymer (53-61%) and magnetite (28-33%) in each complex (Table 6) were comparable to each other, indicating that percentage of each component in the dispersible complexes was not dependent on the structure of the copolymer used.

TGA thermograms of the sat-coated particle shows a consistent weight loss ranging between 130 and 550°C (Figure 42), attributed to the decomposition of organic components including the copolymers and oleic acid complexing to the particle surface. The unsat-coated particle exhibited a first weight loss ranging between 100 to 200°C attributed to the decomposition of maleic components in the complex [52]. This was also observed in the crosslinked-coated particle at the same temperature range. The second major weight loss (250-350°C) was attributable to oleic acid remaining in the complex, which was also observable in same range to those of the oleic acid-coated particle. The weight loss at high temperature ranging between 370 and 470°C was attributed to the decomposition of mPEG in the copolymer [53].

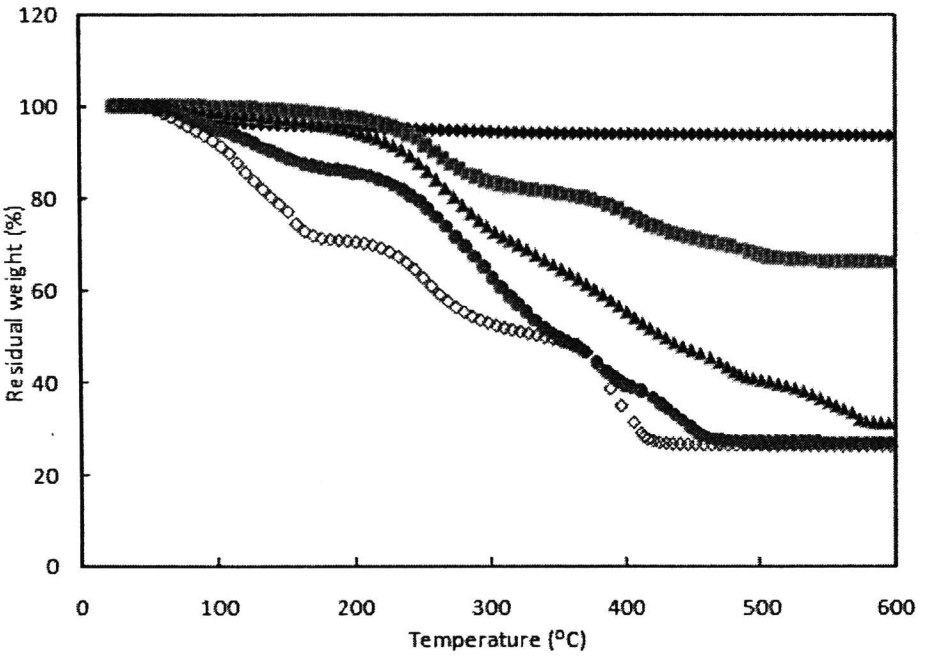

Figure 42 TGA thermograms of bare magnetite (◆), oleic acid-coated magnetite (■), sat-coated particle (▲), unsat-coated particle (●) and crosslinked-coated particle (◇)

Table 6 Percentage of the compositions in oleic acid-coated and copolymer-coated magnetite nanoparticle

	Char yield (%)[a]	Composition in the complexe (%)[d]		
		Fe_3O_4[b]	Oleic acid	Copolymer
Bare particle	93	100	-	-
Oleic acid-coated particle	66	71[c]	29[c]	-
Sat-coated particle	31	33	14	53
Unsat-coated particle	27	29	12	59
Crosslinked-coated particle	26	28	11	61

หมายเหตุ: [a]Assumimg that char yield is the %wt of iron oxide completely oxidized at 600 °C

[b]Assuming that all iron oxides are in the form of Fe_3O_4 at ambient temperature. %Fe_3O_4 is %char yield normalized with 0.93 factor (%char yield of bare magnetite)

[c]Ratio of Fe_3O_4 to oleic acid is 2.4 :1 and this is used to calculate their ratio in other complexes

[d]Total compositions of all components in the complexes are 100%

5. Determination of magnetic properties of the copolymer–magnetite complex via Vibrating Sample Magnetometry (VSM)

A representative hysteresis curve of the unsat-coated particle was shown in Figure 43. It exhibited superparamagnetic behavior at room temperature as indicated by the absence of reminance and coercivity upon removing an external applied magnetic field with the saturation magnetization (M_s) about 9 emu/g. Other complexes, e.g. the sat-coated particle and the crosslinked-coated particle, also showed similar magnetic behavior and M_s value. The observed low M_s value was attributed to the existence of high percentages of the copolymers, as indicated by TGA experiments, which resulted in a low magnetite content in the complexes. It should be

noted that, although their M_s value was low, these copolymer-magnetite complexes still possessed a good responsiveness to an external magnetic field induction.

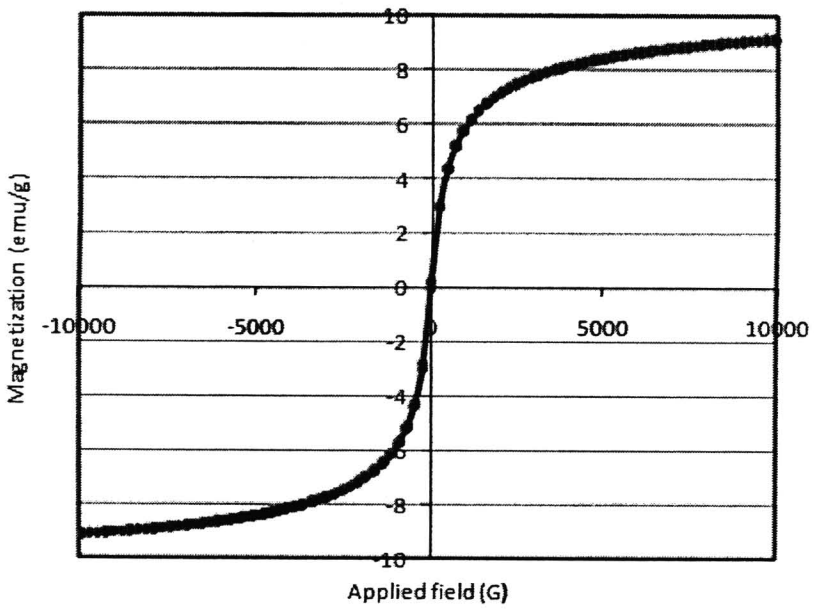

Figure 43 An *M-H* curve of the nanoparticle stabilized with the unsat-coated particles

6. Effect of the copolymer composition on stability of the particles

Figure 44 shows the concentrations of the particles remaining dispersible in water after 1-4 weeks as compared to their initial concentrations. The initial concentrations of the dispersible particles in water were strongly dependent on type of the complexes used. In general, the concentrations of magnetite in water decreased about 10-35% in the first week and continuously dropped to about 50% after four weeks, depending on type of the complexes used. The dispersions containing high magnetite concentrations exhibited high tendency of particle aggregation (about 35% particle aggregation in the first week) due to the great proximity of each particle in the dispersion, resulting in a significant drop of the percentage of the dispersible particles. The dispersions with diluted particle concentrations showed a good stability in water with less than 10% of particle aggregation after one week. However, about 50% of particle aggregation was observed after four weeks of their preparation, indicating that

these complexes might be suitable for short-term uses. The decrease of the dispersible particles in water was attributable to redissolution of the copolymers in the complex to the solution.

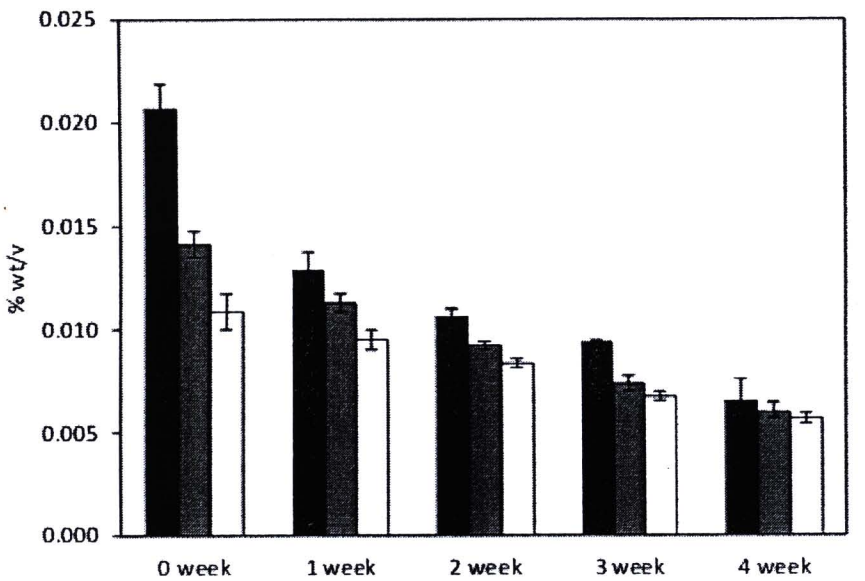

Figure 44 Stability of sat-coated particle (■), unsat-coated particle (■) and crosslinked-coated particle (□) in water at room temperature

7. Indomethacin entrapment and loading efficiencies and its releasing behavior of the copolymer-magnetite complexes

In this experiment, indomethacin entrapment efficiency (%EE) and loading efficiency (%DLE) were investigated to confirm the presence of bilayer surfactant with a hydrophobic inner layer and hydrophilic corona. Indomethacin was selected as a model drug in the current studies due to its poor solubility in water. It was hence conceived that, once the hydrophobic indomethacin was added to the aqueous dispersion, it would somewhat partition to the inner hydrophobic shell (oleic acid-polyester layer) of the complex. In the present work, different structures of the polyester inner layer, e.g. saturated, unsaturated and crosslinked polyesters, were designed in order to investigate the effect of its structure on entrapment and loading efficiencies of an indomethacin model drug.

According to the results in Figure 45, %EE in these complexes ranged between 48 and 82% (48-82 mg indomethacin entrapped/100 mg indomethacin loaded), while %DLE ranged between 61 and 97% (610-970 μg/mg Fe_3O_4). Both %EE and %DLE in the sat-coated particle were significantly higher than those of the unsat-coated particles. The decreases in %EE and %DLE in the unsat-coated particle were attributed to the relatively high polarity of double bonds in the unsaturated polyester, resulting in the suppression of the entrapment and loading efficiencies of the hydrophobic drug in the polyester layer. %EE and %DLE in the case of the crosslinked-coated particle show higher values than those of the unsat-coated one (before crosslinking reaction). It should be noted that the crosslinking reaction was performed after drug loading process; the drug can be entrapped in the network structure, resulting in the promotion of the drug loading and entrapment efficiencies. An example of the calculations is shown in Appendix A-6 and A-7.

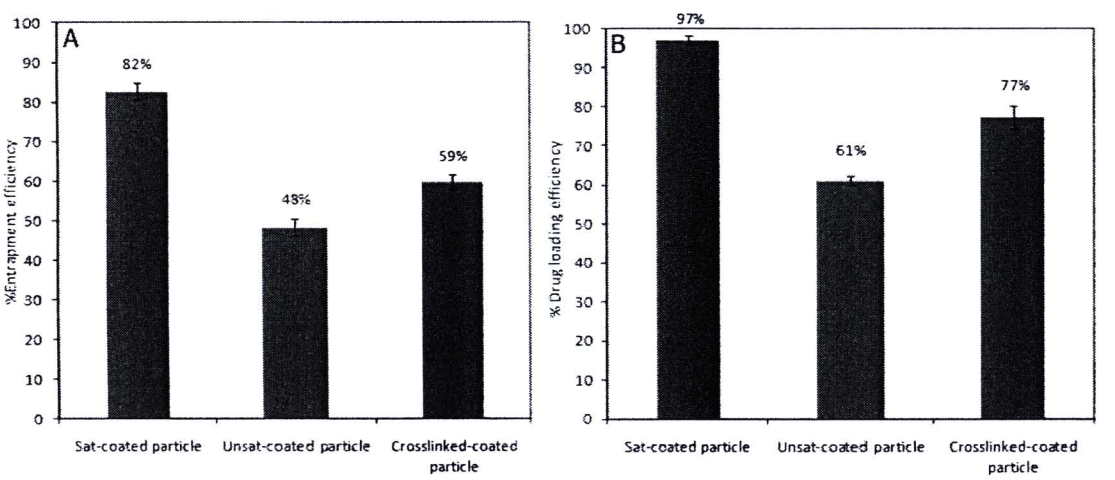

Figure 45 (A) Indomethacin entrapment efficiency (%EE) and (B) drug loading efficiency (%DLE) of the copolymer-magnetite complexes

Releasing behavior of indomethacin entrapped in the copolymer-coated particles was investigated in phosphate buffer solution (PBS). Suspension of the particles in water was dialyzed in PBS releasing media with pH 7.4. Concentrations of indomethacin released from the suspension in PBS releasing media were analyzed at a

given time until % release reached its equilibrium. According to the results in Figure 46, % drug release of the sat- and unsat-coated particles reached their equilibriums within 3 h of dialysis, whereas those of the crosslinked-coated particle was about 8 h of dialysis, implying that crosslinking of the polyester inner shell was able to sustain the releasing rate of the entrapped drug from the complexes. Low percent drug released at equilibrium (45%) was again attributed to the crosslinked structure of polyester, which might inhibit the releasing efficiency of the drug from the complexes. Percentages of drug released at equilibrium of the sat- and unsat-coated particles were 88% and 62%, respectively. The relatively high percent drug released at equilibrium of the sat-coated particle was attributable to the high %EE and %DLE of this complex as compared to those of the unsat-coated one, resulting in a high amount of the drug to be released from the complex.

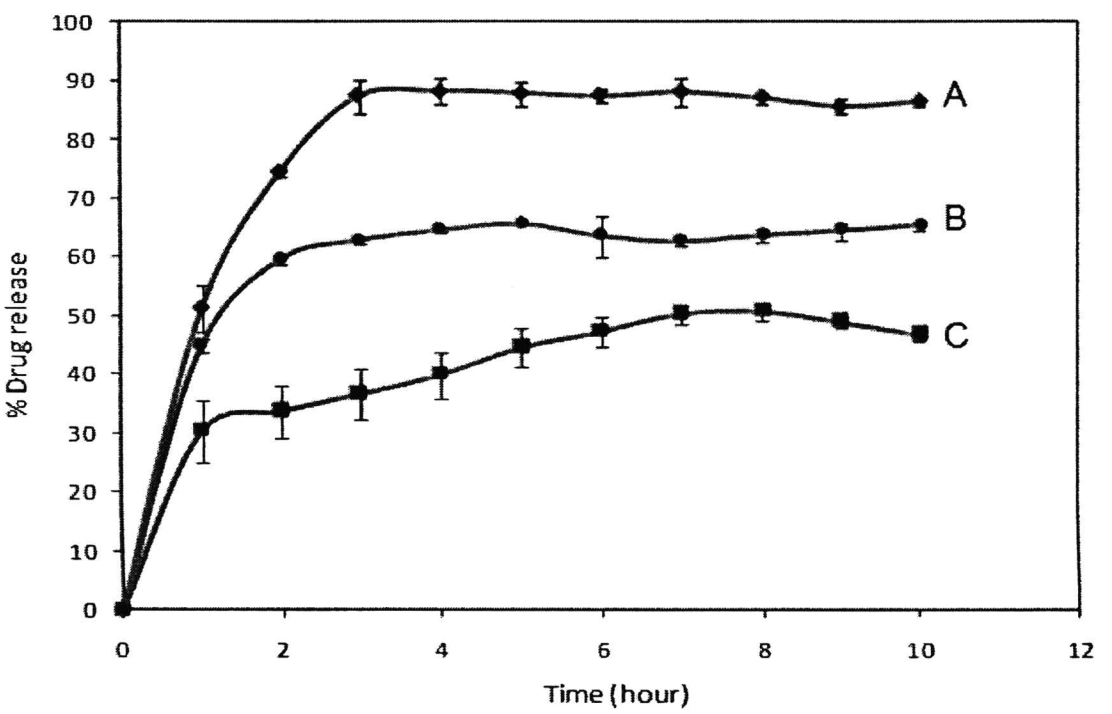

Figure 46 Indomethacin-released profiles of (A) the sat-coated particle, (B) the unsat-coated particle and (C) the crosslinked-coated particle